**Attenuation of Inhibitory PGE2 Signaling in Human Lung Fibroblasts is Mediated by PDE4**

Joel Michalski, Nobuhiro Kanaji, Xiangde Liu, Steve Nogel, Xingqi Wang, Hesham Basma, Masanori Nakanishi, Tadashi Sato, Yoko Gunji, Maha Fahrid, Amy Nelson, Kai-Christian Muller, Olaf Holz, Helgo Magnussen, Klaus F. Rabe, Myron L. Toews, and Stephen Rennard

**Supplemental Text**

**Mechanisms involved in the regulation of attenuated PGE2 signaling following PGE2 pretreatment.**

PGE2 was added to HFL cells at different time points with a final pretreatment concentration of 0.1 μM. Following the maximal pretreatment time point (12 hr), cells were harvested, suspended in SF medium with or without PGE2 (0.1 μM) and chemotaxis assessed (**Supp Fig 1a**). Loss of PGE2-mediated inhibition of migration was induced by four hours of pretreatment. However, increased baseline chemotaxis trended to take longer (4-12 hrs) to develop, suggesting separate mechanisms may account for these two phenomena.

To assess if the time-dependent loss of PGE2-mediated inhibition of chemotaxis is associated with attenuated cAMP accumulation, inhibition of cAMP production was assessed as a function of time of pretreatment with PGE2. HFL cells were cultured in SF media for 30 minutes, after which the media were replaced with fresh SF medium. At the appropriate time point (from 4 hours up to 30 minutes prior to assessment) PGE2 was added to the wells for a final pretreatment concentration of 0.1 μM. Following pretreatment, PGE2-mediated cAMP accumulation was assessed (**Supp Fig 1b**). Cells receiving only a short-term pretreatment with PGE2 (30 minutes to 1 hr) did not exhibit attenuated cAMP accumulation when further stimulated with PGE2. However, attenuation was observed after two hours and increased up to 4 hours (**Supp Fig 1b**), correlating with the time course for loss of inhibition of chemotaxis. These time frames suggest that receptor phosphorylation and uncoupling are unlikely involved, as these mechanisms typically occur more rapidly (minutes) in GPCRs (1-4).

The time required to reverse the effect of PGE2 pretreatment was also evaluated. Cells were pretreated with PGE2 (0.1 μM) for 24 hours. PGE2 was removed at varying time points and cells washed twice with SF media. Complete recovery took roughly seven hours (**Supp. Fig. 1c**). Again, this time frame suggests mechanisms other than receptor uncoupling mediated by phosphorylation and supported by the absence of receptor down-regulation detectable by western blot (**Supp. Fig. 2d**).

To determine if PGE2 responses were lost or only relatively less sensitive to PGE2 signaling following 24-hour PGE2 pretreatment, experiments were performed where the concentration of ligand used to stimulate control and PGE2 pretreated cells was increased. Following a fixed concentration of PGE2 (0.1 μM) pretreatment, the response to PGE2 was attenuated, but higher concentrations of PGE2 were able to inhibit chemotaxis (**Supp Fig 2a**) in a concentration-dependent manner. This effect was mediated by the EP2 receptor (**Supp. Fig. 2c**). Similar experiments were performed for PGE2-stimulated cAMP accumulation. As with chemotaxis, PGE2 pretreatment resulted in an attenuated response, but PGE2 at higher concentrations exhibited a concentration-dependent stimulation of cAMP accumulation **(Supp. Fig. 2b)**. In addition, levels of EP receptors remain unchanged following PGE2 pretreatment, ruling out receptor down-regulation (**Supp. Fig. 2d**). These data suggest that PGE2 receptors remain present and functional but that the pretreated cells have developed a relative *resistance* to PGE2-mediated cAMP accumulation and inhibition of chemotaxis.

Transfection of HFL fibroblasts with pooled PDE4A-C reduced expression of both PDE4A and PDE4C (**Supp. Fig 3a**), but not PDE4B. Cells transfected with non-targeting siRNA and pretreated with PGE2 developed resistance to PGE2-mediated inhibition of chemotaxis, as expected. Cells transfected with pooled PDE4A-C siRNA's prior to pretreatment with PGE2 remained sensitive to inhibition of chemotaxis

by PGE2 (**Supp. Fig 3b**). Pooled PDE4 siRNA transfection was also associated with restored PGE2-mediated cAMP accumulation (**Supp. Fig 3c**).

Transfection with single PDE4 siRNA constructs was performed to determine which specific isoform of PDE4 is mediating attenuation of PGE2 signaling following PGE2 pretreatment (**Supp. Fig 4a-c**). Transfection with individual siRNAs at a single concentration (300 nM) of each PDE4 isoform detected by western blot (individual PDE4A, B and C constructs) failed to prevent attenuation of PGE2 signaling following PGE2 pretreatment. Transfection with PDE4A and PDE4C siRNA in combination prior to PGE2 pretreatment was able to block loss of PGE2-mediated inhibition of chemotaxis (**Supp. Fig 4d**) and was also associated with a numerical restoration of PGE2 mediated cAMP accumulation (**Supp. Fig 4e**). This suggests that the PDE4A and PDE4C isozymes are the key enzymes that mediate loss of PGE2-mediated signaling following PGE2 pretreatment and likely function in a redundant manner.

As presented in the main text in figures 5a and 5b, we also calculated an index of inhibition to make direct comparisons between fibroblasts obtained from both COPD and normal lungs and display inter-subject variability (Supp. Fig 5a-b). In normal fibroblasts, PGE2 pretreatment resulted in a decreased ability of PGE2 to inhibit chemotaxis, a result similar to findings observed in HFL fibroblasts. COPD cells, however, did not develop attenuated inhibitory PGE2 signaling (Supp Fig 5a). The change in PGE2 inhibition indexes following 24 hour PGE2 pretreatment is displayed in Supp Fig 5b. COPD fibroblasts did not undergo attenuation of inhibitory PGE2 signaling following PGE2 pretreatment and this was significantly different when compared directly to normal fibroblasts.

**Supplemental Text Works Cited**

1. Hausdorff WP, Bouvier M, O'Dowd BF, Irons GP, Caron MG, Lefkowitz RJ. Phosphorylation sites on two domains of the beta 2-adrenergic receptor are involved in distinct pathways of receptor desensitization. J Biol Chem 1989 Jul 25;264(21):12657-65.

2. Nishigaki N, Negishi M, Ichikawa A. Two gs-coupled prostaglandin E receptor subtypes, EP2 and EP4, differ in desensitization and sensitivity to the metabolic inactivation of the agonist. Mol Pharmacol 1996 Oct;50(4):1031-7.

3. Desai S, April H, Nwaneshiudu C, Ashby B. Comparison of agonist-induced internalization of the human EP2 and EP4 prostaglandin receptors: Role of the carboxyl terminus in EP4 receptor sequestration. Mol Pharmacol 2000 Dec;58(6):1279-86.

4. Kassis S, Fishman PH. Functional alteration of the beta-adrenergic receptor during desensitization of mammalian adenylate cyclase by beta-agonists. Proc Natl Acad Sci U S A 1984 Nov;81(21):6686-90.

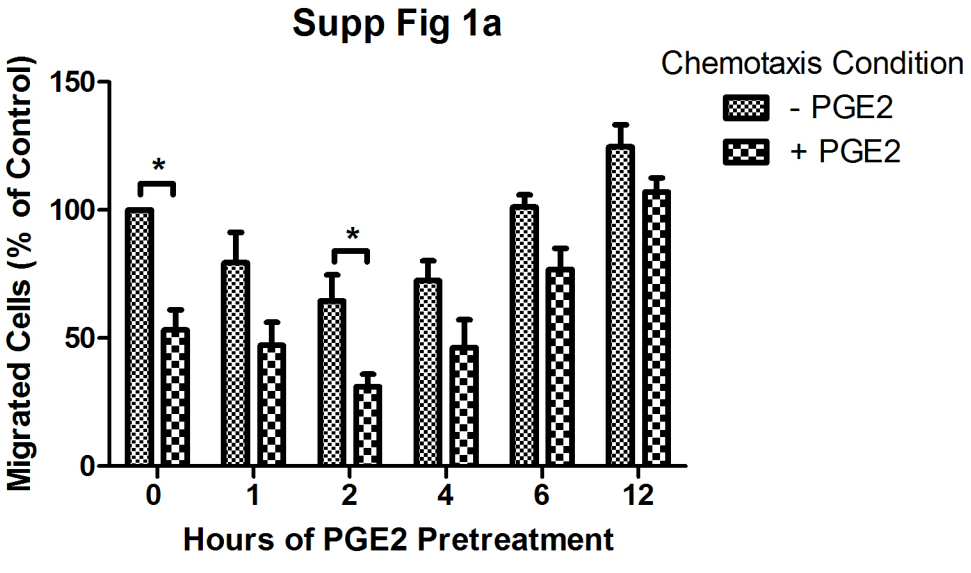
Supp Fig 1a
Chemotaxis Condition
- PGE2
+ PGE2
Migrated Cells (% of Control)
150
100
50
0
*
*
0
1
2
4
6
12
Hours of PGE2 Pretreatment

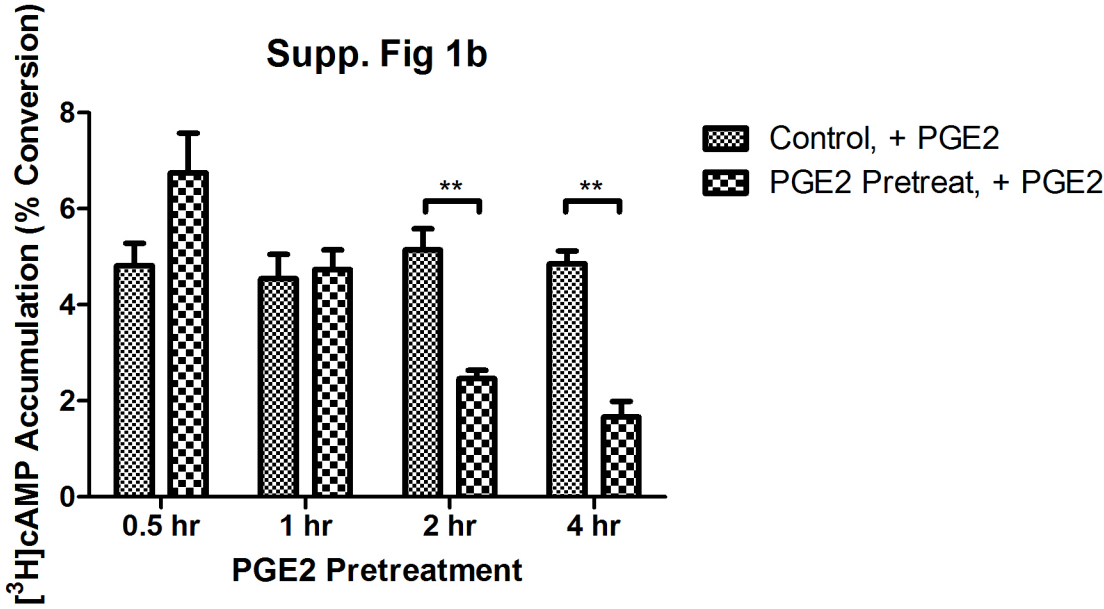
Supp. Fig 1b
[3H]cAMP Accumulation (% Conversion)
8
6
4
2
0
**
**
0.5 hr
1 hr
2 hr
4 hr
PGE2 Pretreatment
Control, + PGE2
PGE2 Pretreat, + PGE2

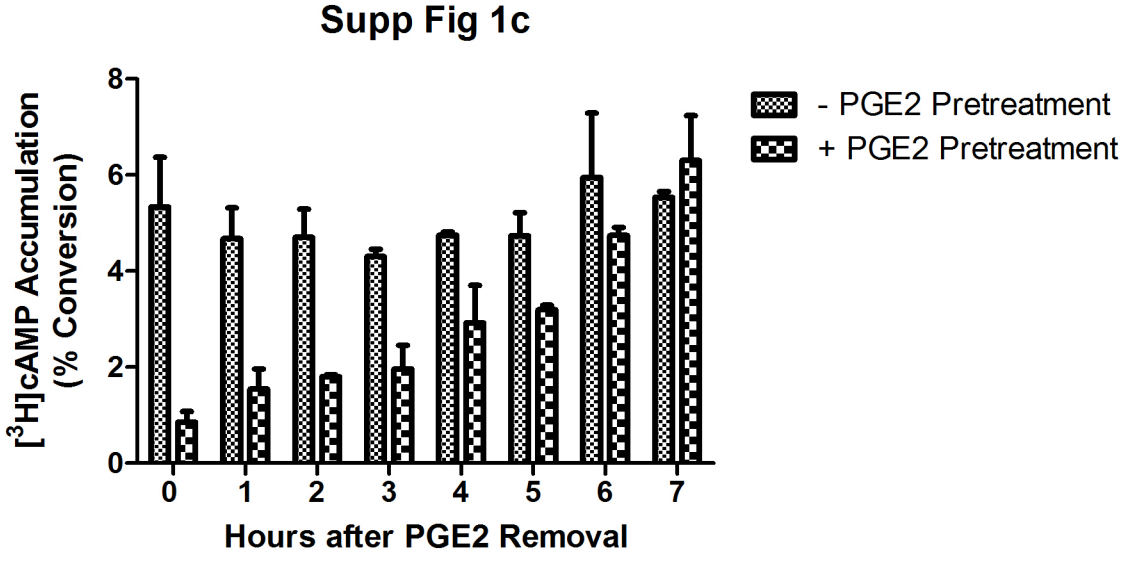
Supp Fig 1c
[3H]cAMP Accumulation (% Conversion)
8
6
4
2
0
0
1
2
3
4
5
6
7
Hours after PGE2 Removal
- PGE2 Pretreatment
+ PGE2 Pretreatment

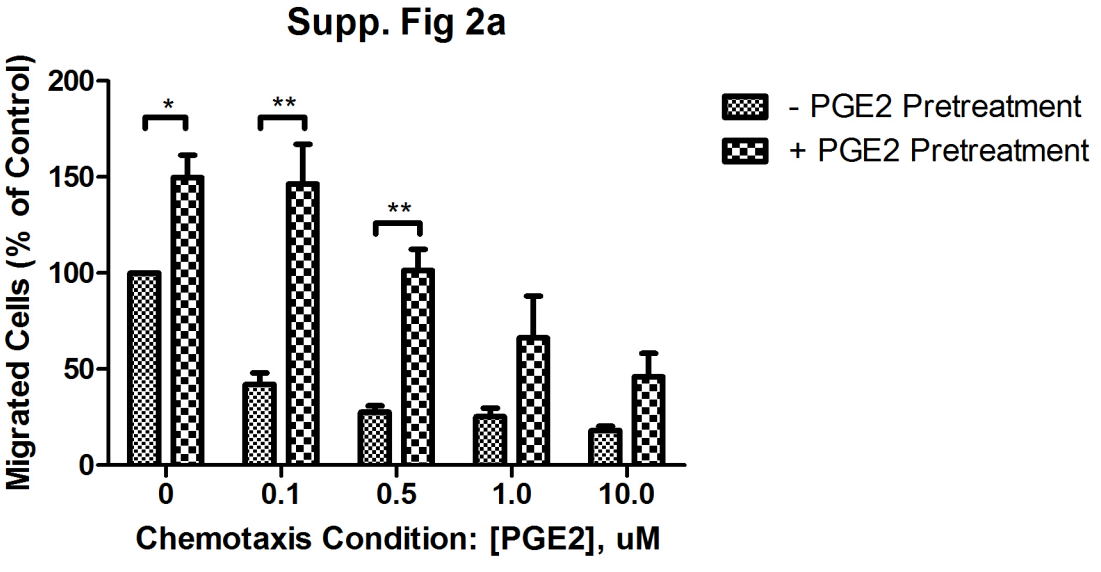
Supp. Fig 2a
Migrated Cells (% of Control)
200
150
100
50
0
*
**
**
0
0.1
0.5
1.0
10.0
Chemotaxis Condition: [PGE2], uM
- PGE2 Pretreatment
+ PGE2 Pretreatment

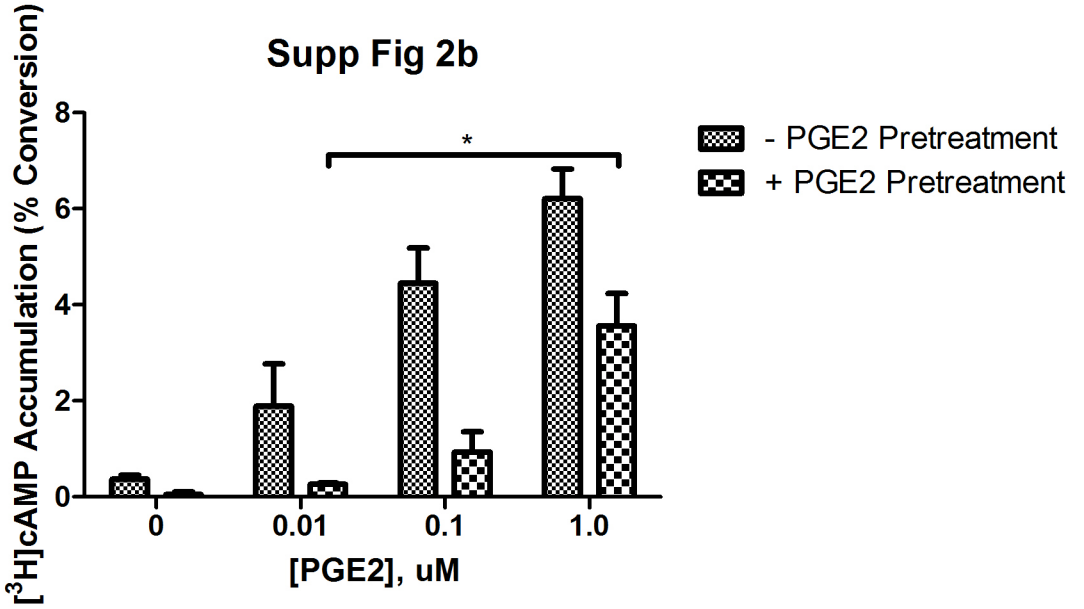
Supp Fig 2b
[3H]cAMP Accumulation (% Conversion)
8
6
4
2
0
*
0
0.01
0.1
1.0
[PGE2], uM
- PGE2 Pretreatment
+ PGE2 Pretreatment

# Supp Fig 2c

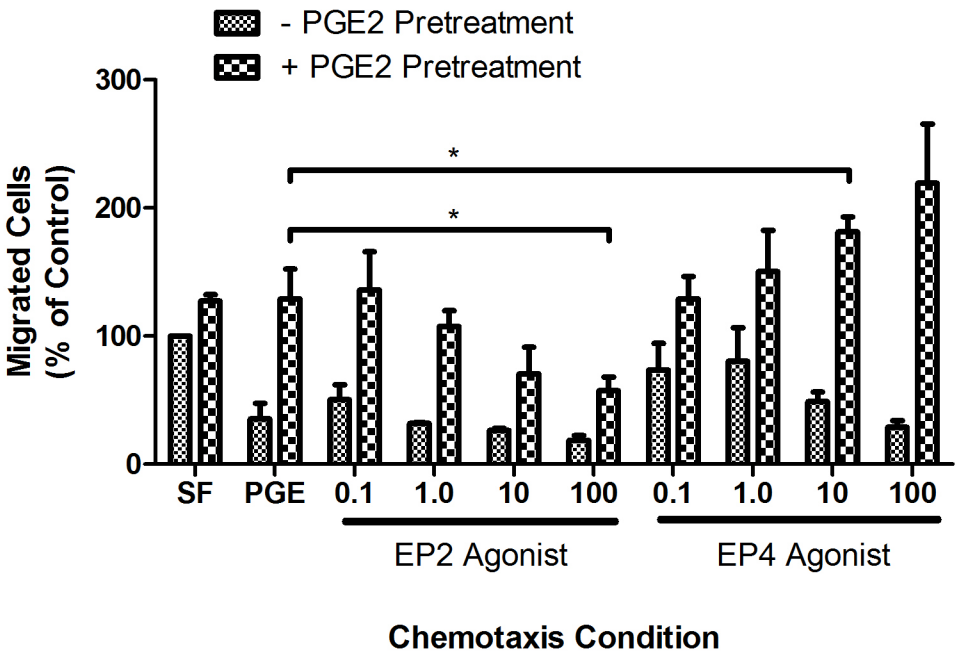
- PGE2 Pretreatment
+ PGE2 Pretreatment
Migrated Cells
(% of Control)
300
200
100
0
*
*
SF
PGE
0.1
1.0
10
100
0.1
1.0
10
100
EP2 Agonist
EP4 Agonist
Chemotaxis Condition

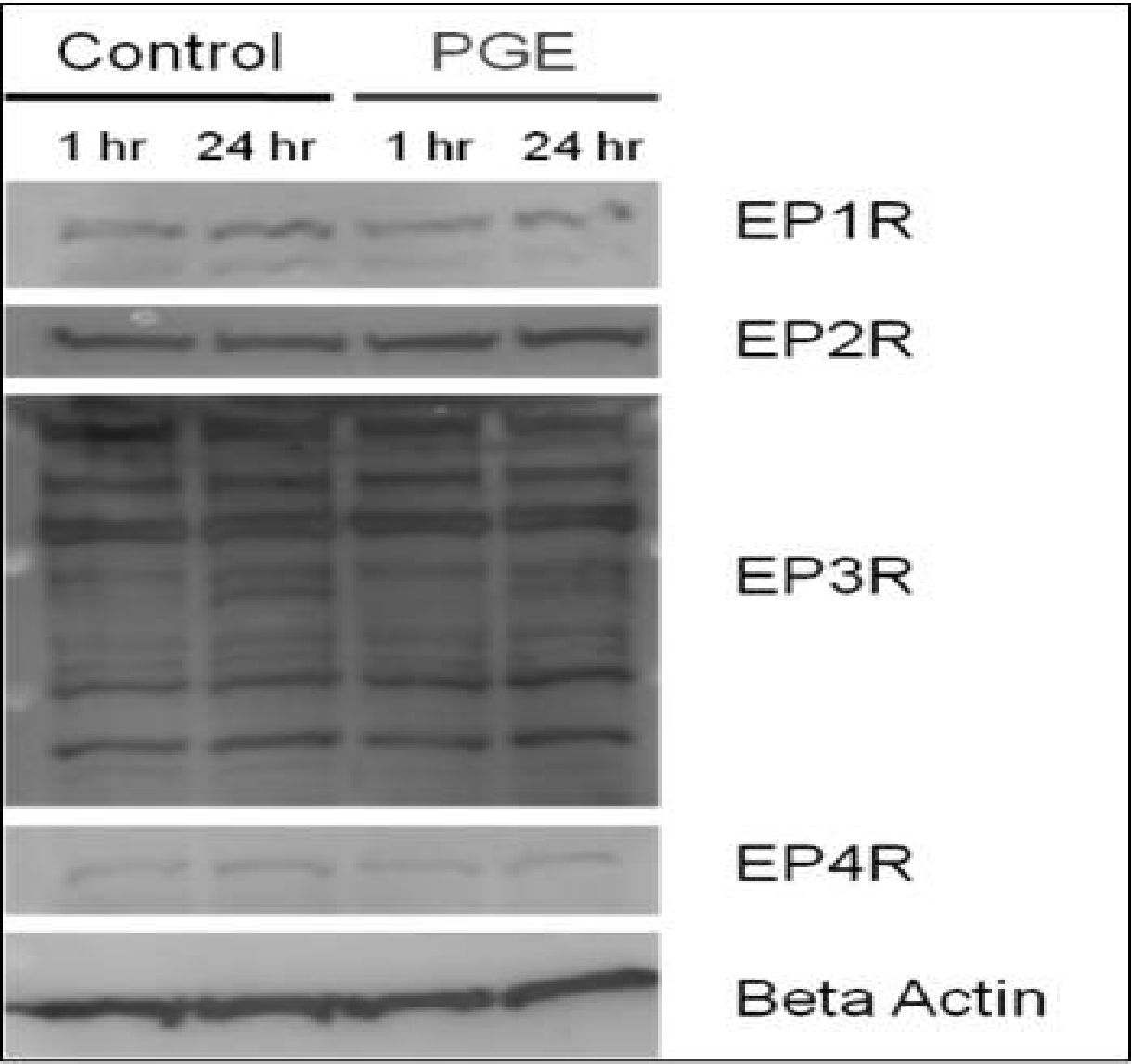
Control
PGE
1 hr
24 hr
1 hr
24 hr
EP1R
EP2R
EP3R
EP4R
Beta Actin

Supp Fig 3a

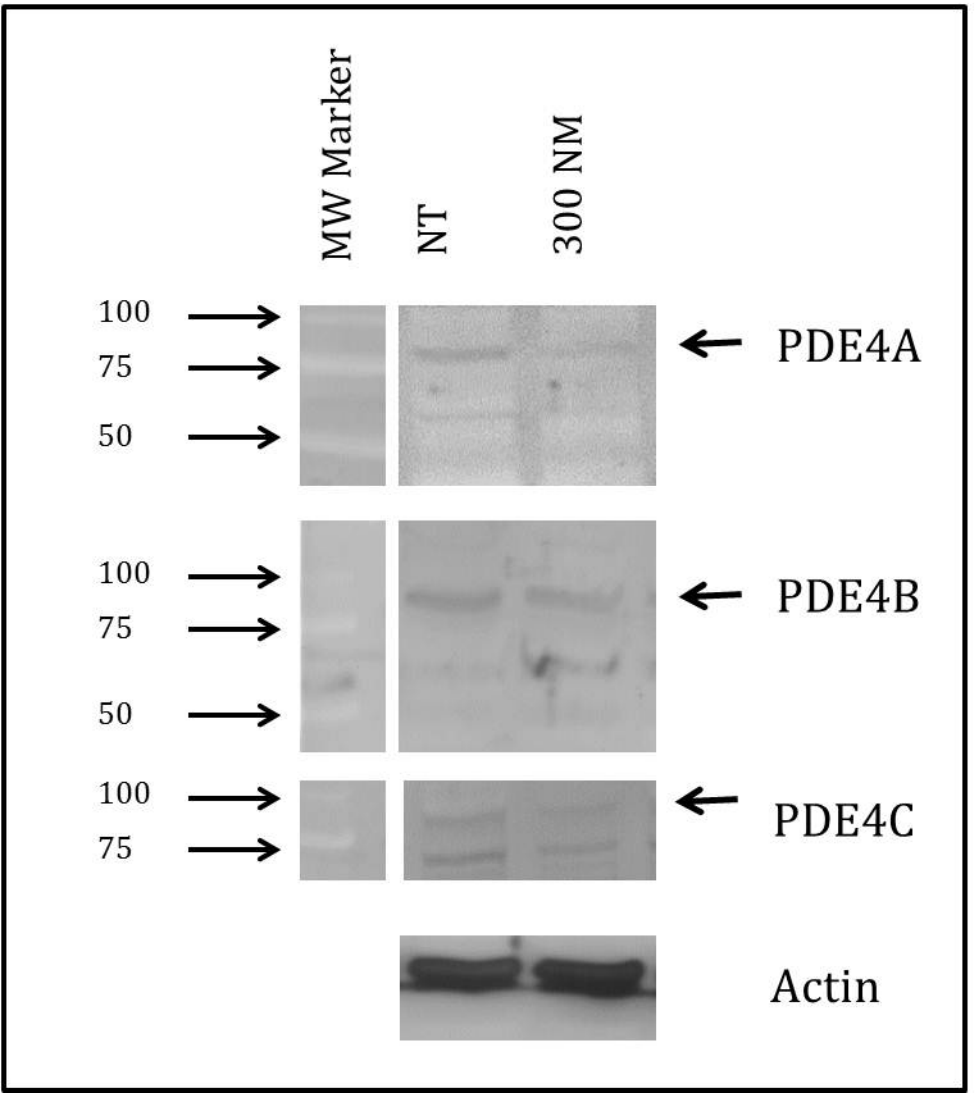
MW Marker
NT
300 NM
100
75
50
PDE4A
100
75
50
PDE4B
100
75
PDE4C
Actin

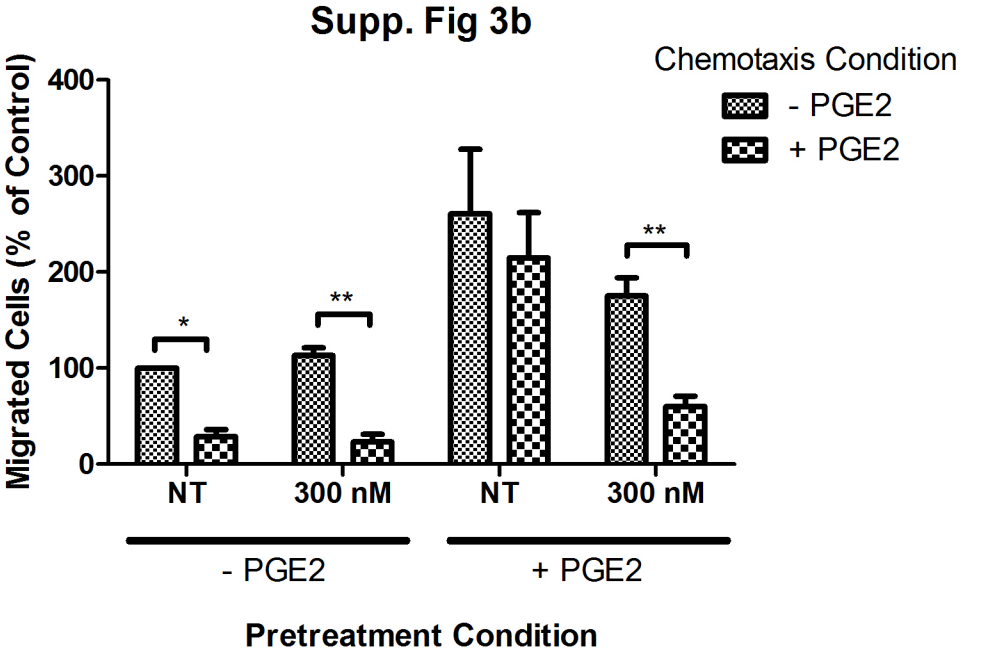
Supp. Fig 3b
Chemotaxis Condition
- PGE2
+ PGE2
Migrated Cells (% of Control)
400
300
200
100
0
*
**
**
NT
300 nM
NT
300 nM
- PGE2
+ PGE2
Pretreatment Condition

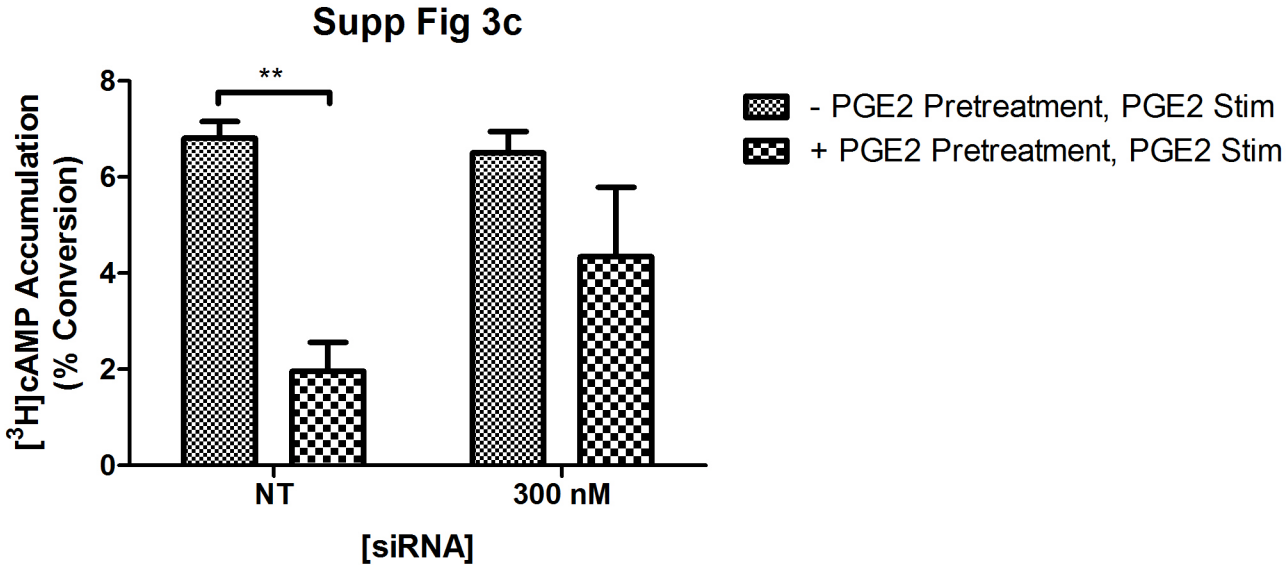
Supp Fig 3c
**
8
6
4
2
0
[3H]cAMP Accumulation
(% Conversion)
NT
300 nM
[siRNA]
- PGE2 Pretreatment, PGE2 Stim
+ PGE2 Pretreatment, PGE2 Stim

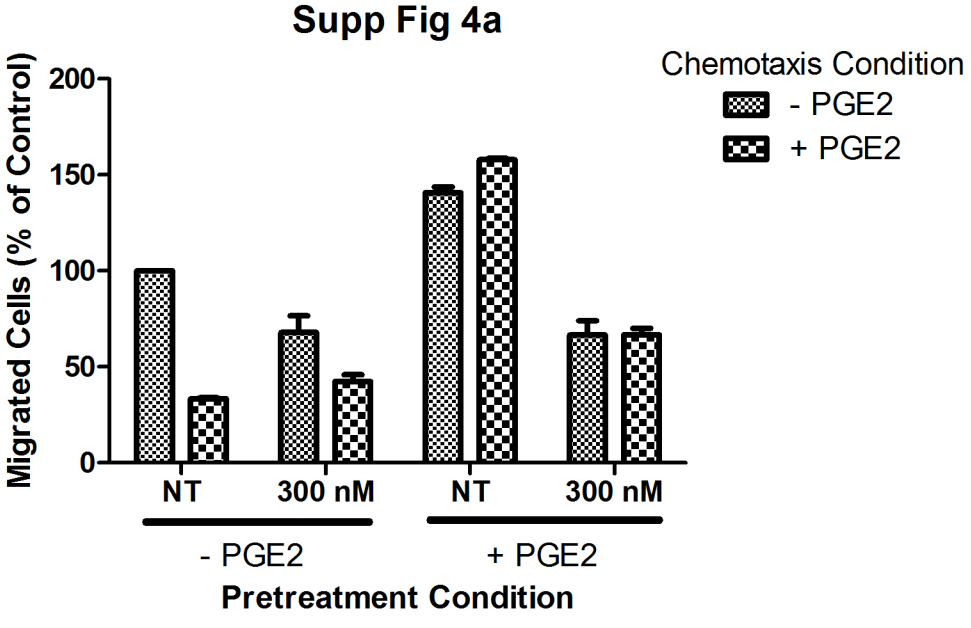
Supp Fig 4a
Chemotaxis Condition
- PGE2
+ PGE2
Migrated Cells (% of Control)
200
150
100
50
0
NT
300 nM
NT
300 nM
- PGE2
+ PGE2
Pretreatment Condition

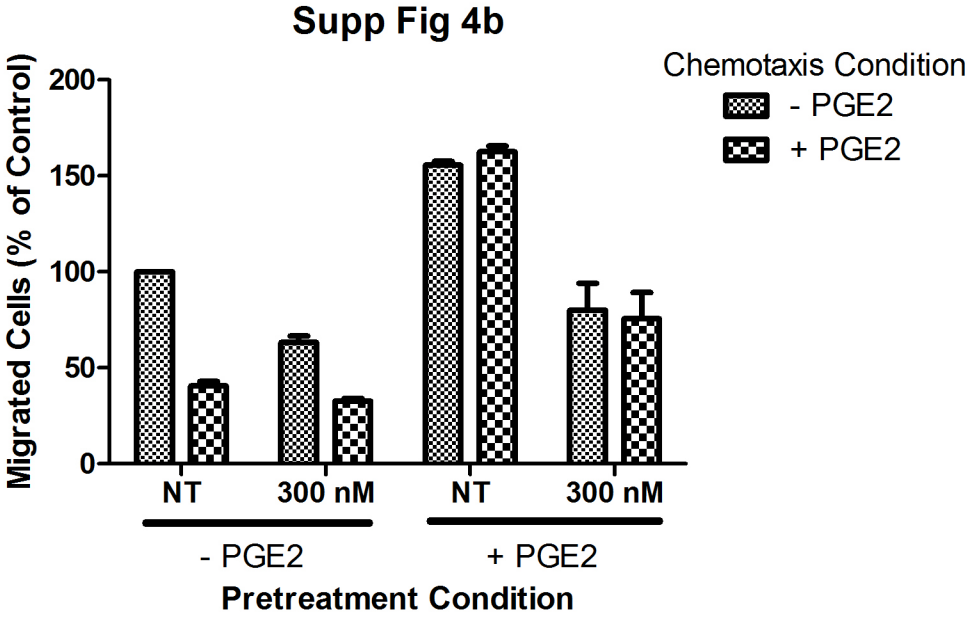
Supp Fig 4b
Chemotaxis Condition
- PGE2
+ PGE2
Migrated Cells (% of Control)
200
150
100
50
0
NT
300 nM
NT
300 nM
- PGE2
+ PGE2
Pretreatment Condition

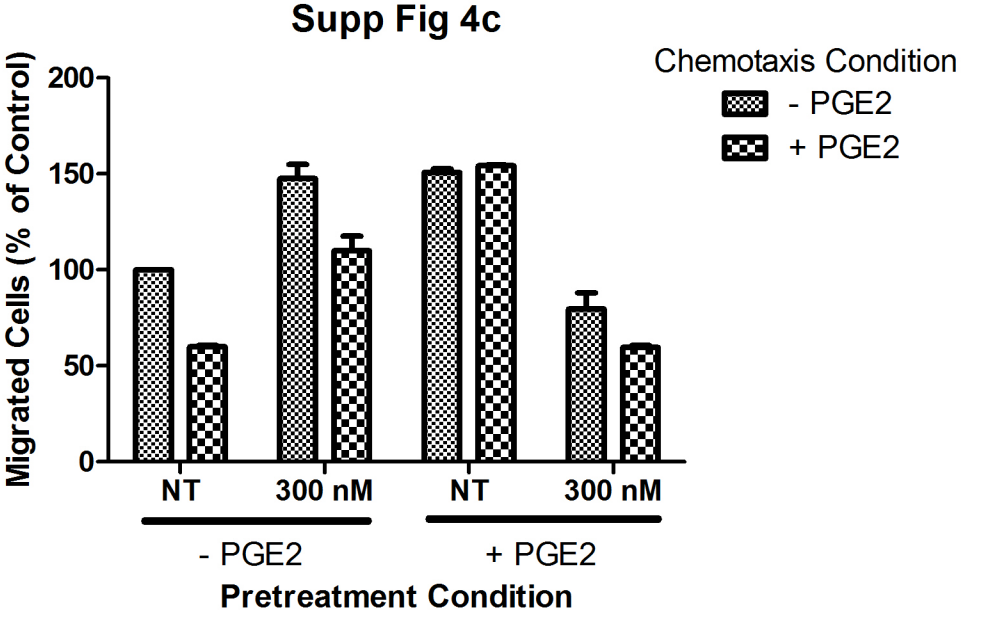
Supp Fig 4c
Chemotaxis Condition
- PGE2
+ PGE2
Migrated Cells (% of Control)
200
150
100
50
0
NT
300 nM
NT
300 nM
- PGE2
+ PGE2
Pretreatment Condition

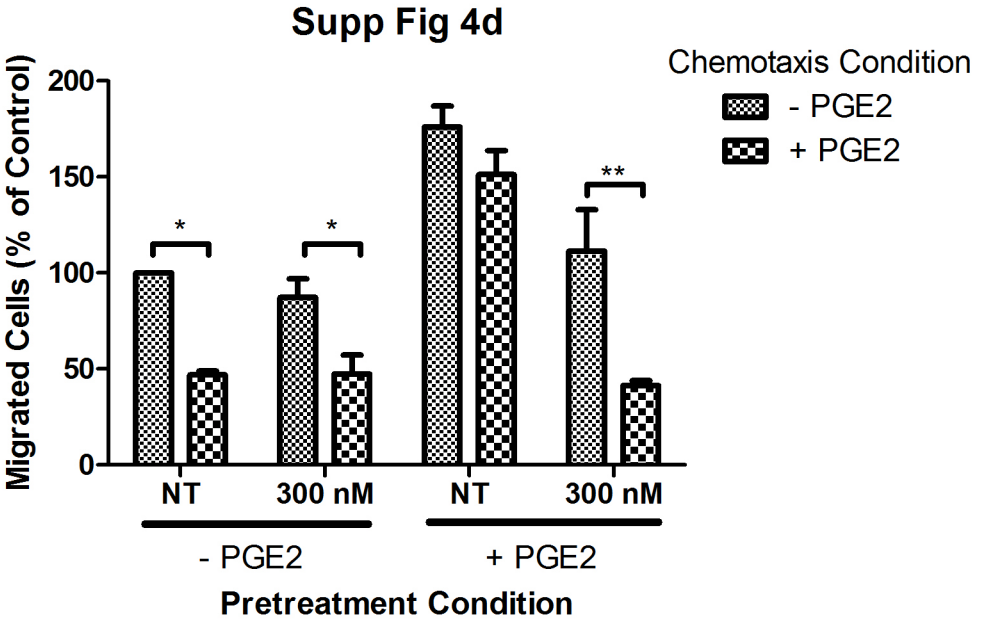
Supp Fig 4d
Chemotaxis Condition
- PGE2
+ PGE2
Migrated Cells (% of Control)
200
150
100
50
0
*
*
**
NT
300 nM
NT
300 nM
- PGE2
+ PGE2
Pretreatment Condition

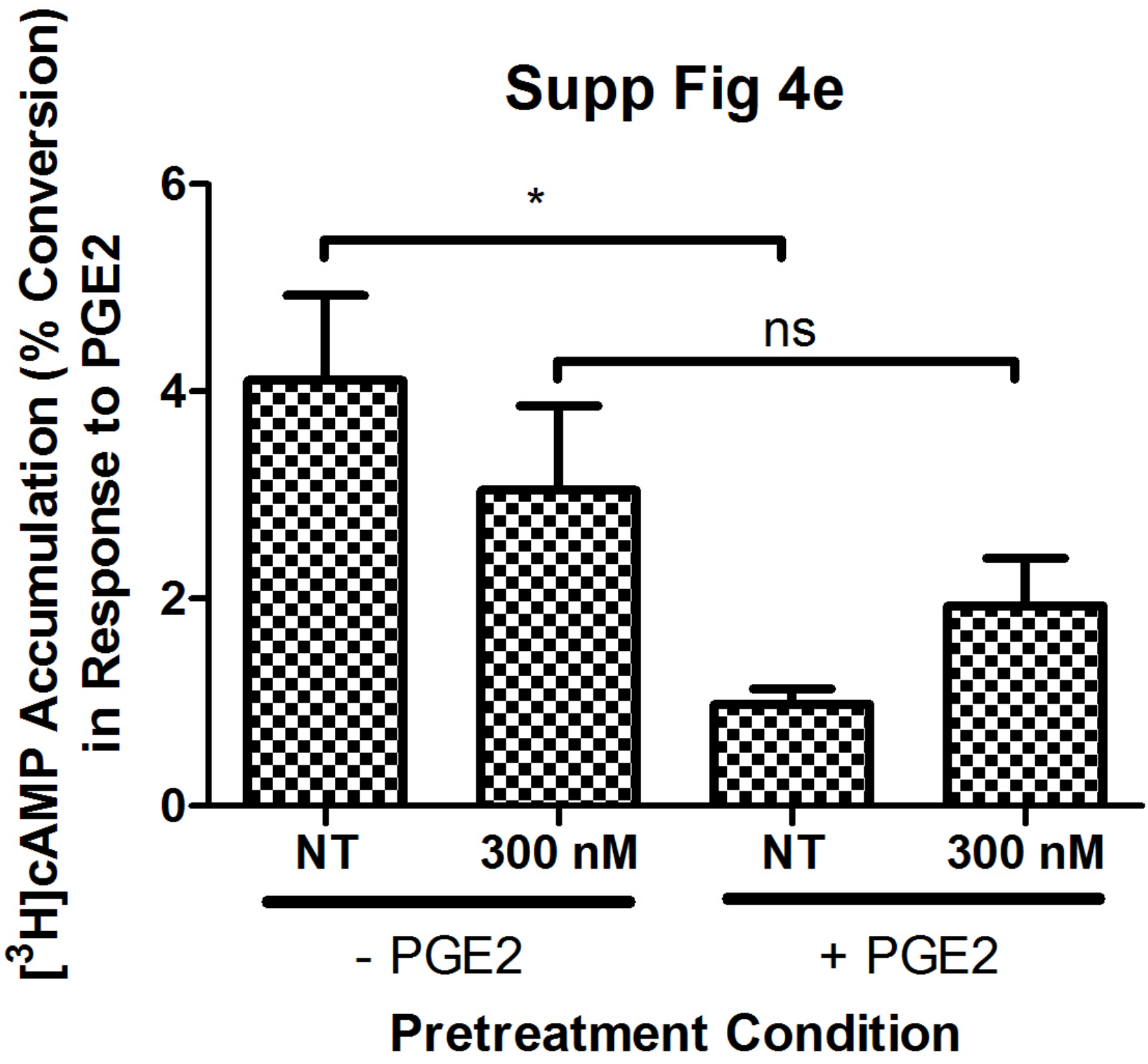
Supp Fig 4e
[3H]cAMP Accumulation (% Conversion) in Response to PGE2
6
4
2
0
*
ns
NT
300 nM
NT
300 nM
- PGE2
+ PGE2
Pretreatment Condition

# Supp. Fig 5a

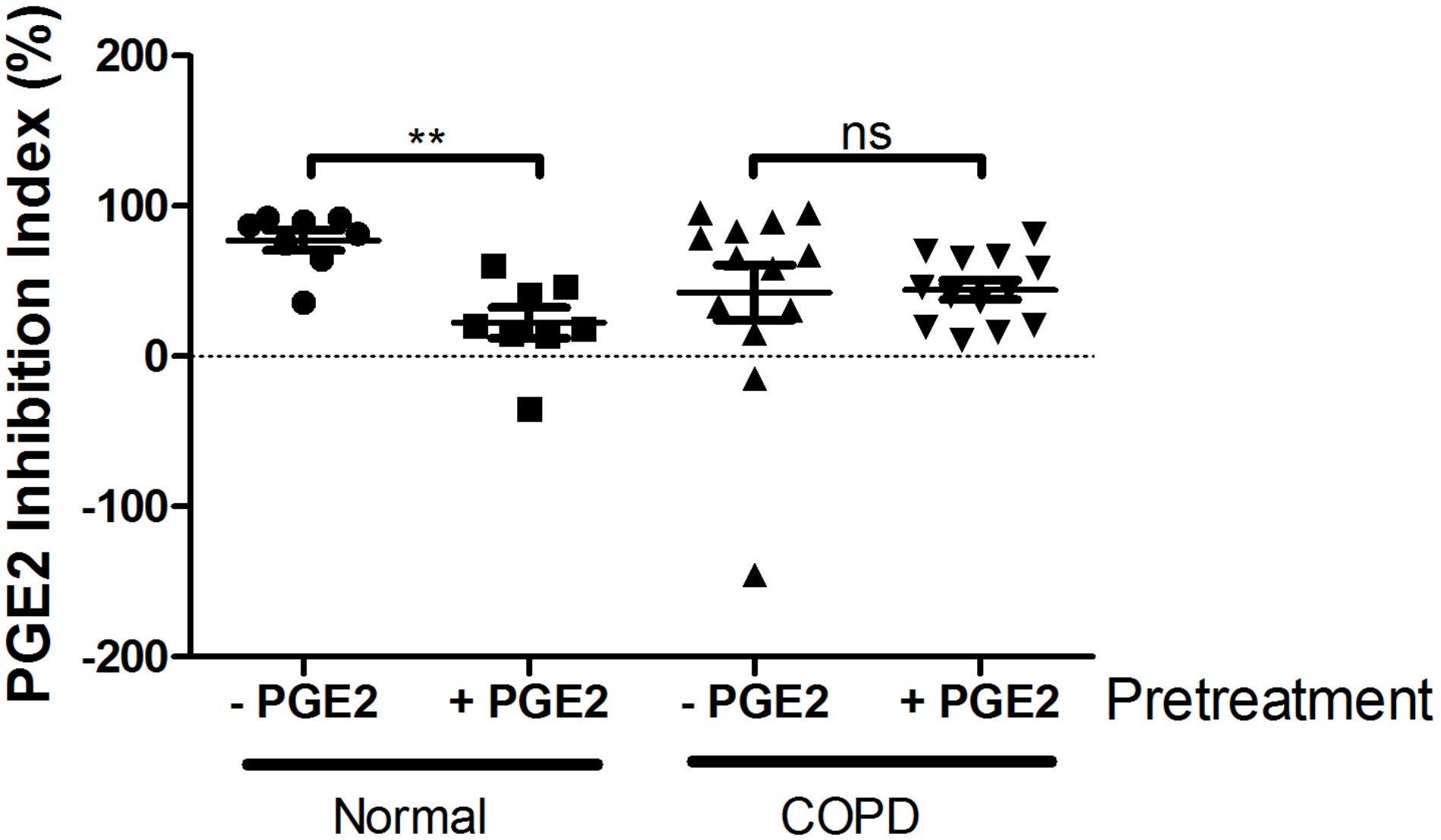
PGE2 Inhibition Index (%)
200
100
0
-100
-200
**
ns
- PGE2
+ PGE2
- PGE2
+ PGE2
Pretreatment
Normal
COPD

# Supp. Fig 5b

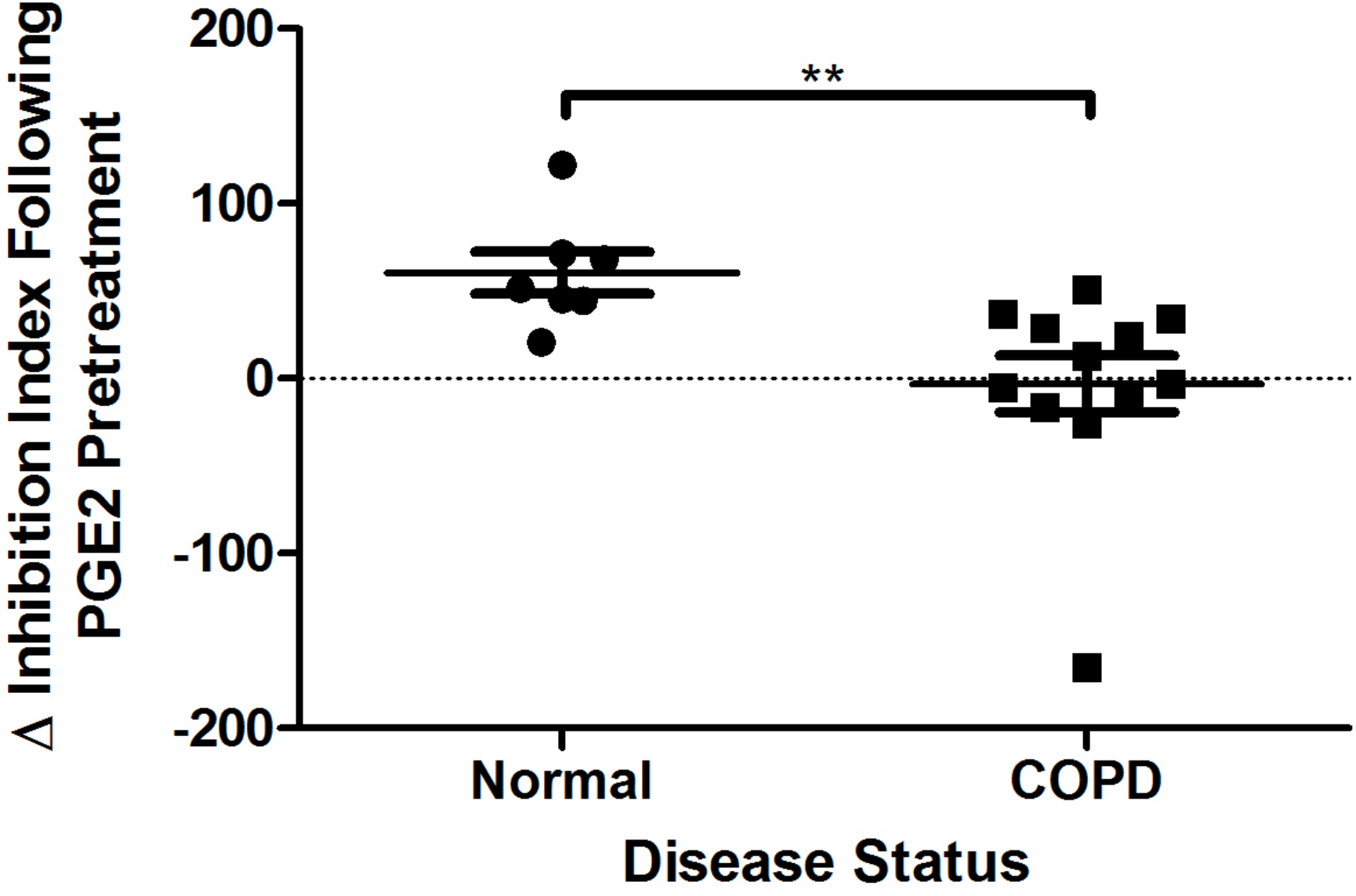
Δ Inhibition Index Following PGE2 Pretreatment
200
100
0
-100
-200
**
Normal
COPD
Disease Status